

## Journal of Advanced Research in Fluid Mechanics and Thermal Sciences

Journal of Advanced Research in Fluid Mechanics and Thermal Sciences

Journal homepage: www.akademiabaru.com/arfmts.html ISSN: 2289-7879

# Effect of Baffle Configuration on Heat Transfer and Pressure Drop Characteristics of Jet Impingement System with Cross-Flow

Sabu Kurian<sup>1,\*</sup>, Tide P. S.<sup>2</sup>, Biju N<sup>2</sup>

- <sup>1</sup> School of Engineering, Cochin University of Science and Technology, Cochin, Kerala, India
- <sup>2</sup> Mechanical Engineering, School of Engineering, Cochin University of Science and Technology, Cochin, Kerala, India

#### **ARTICLE INFO ABSTRACT** Article history: Use of baffles in jet impingement systems in presence of initial cross-flow disturbs Received 7 June 2021 boundary layer that results in rise in heat transfer. Two configurations of baffle assisted Received in revised form 8 July 2021 impingement systems were considered and a comparative study on heat transfer and Accepted 15 July 2021 pressure drop is carried out based on operating parameters such as baffle clearance, Available online 19 August 2021 blow ratio and h/D ratio using commercially available CFD package. Numerical predictions showed that both heat transfer and pressure drop in segmented configuration were higher than louvered configuration for all blow ratio employed in this study. Parametric studies showed that, thermo-hydraulic performance parameter is higher only for louvered configurations at low blow ratio. When cross-flow velocity is comparable with jet velocity, segmented baffles resulted in relatively higher thermohydraulic performance because of its higher heat transfer rate relative to the incurring pressure drop. An increase in clearance proportionally increases performance Kevwords: parameter. However, as jet to plate distance increases, thermo hydraulic performance Jet impingement; ross-flow; segmented; declines significantly. louvered

## 1. Introduction

Jet impingement is a promising technology with high relevance because of its intense heat transfer characteristics. It is the technology which offers best heat transfer among similar single phase heat transfer system. The technology has attracted the attention of thermal engineers because of its applicability in situations with high heat flux and limited space. It has versatile applications in various engineering arenas such as electronic cooling, heat treatment of metals, drying of food stuff, and paper etc.

Investigation in jet impingement has started long back from 1951 by Friedman and Mueller [1]. Their experiment was on single jet and since then many researchers had attempt with experimental and analytical approach with an objective to furnish mathematical and graphical enabled solution for heat transfer. Jambunathan *et al.*, [2] carried out experimental study on turbulent impinging jets with Reynolds number ranges up to 1,24,000 and observed four different flow regimes for an impinging

E-mail address: sabukurian74@gmail.com

https://doi.org/10.37934/arfmts.86.2.1527

.

<sup>\*</sup> Corresponding author.



round jet on a flat plate. They are potential core, developing and developed flow zone, stagnation zone, and wall jet zone. Investigations of Gauntner *et al.*, [3] revealed that length of potential core extends up to six times nozzle diameters from jet exit plane. At the stagnation region, they observed rapid decrease in axial velocity and increase in static pressure. Tani and Komatsu [4] observed that the stagnation region expands up to two times nozzle diameters on the flat surface. They reported that, rapid increase of local fluid velocity at the beginning of wall jet zone reaches a maximum and then decrease with distance from the nozzle axis. Wall jet interaction with the surrounding fluid augments the fluid turbulence, which is the major reason for heat transfer in this zone.

Goldstein et al., [5] conducted experimental investigation on local heat transfer from a target plate to an air jet for h/D ranges from 2 to 12. They observed that, up to h/D = 6, heat transfer in the wall jet area is dependent of nozzle plate to target plate distance ratio. Hollworth and Wilson [6] reported that jet Reynolds number is directly proportional to the heat transfer in a jet impingement system. Hansen and Webb [7] investigated the heat transfer characteristics of an air jet impinging on a finned target plate. The average Nusselt number is found to be enhanced by 12% to 33% for short square, pyramidal, and intermediate square fins.

Weigand and Spring [8] conducted an elaborate study on heat transfer characteristics of array of impinging air jets and correlated that with impinging single jet. They studied about the heat transfer influencing factors such as cross-flow, jet Reynolds number, jet pattern, and h/D ratio. They studied different CFD models for best prediction of heat transfer rate of a multi-jet impingement system.

It is established that cross-flow deteriorates heat transfer due to the phenomena of jet sweep-away and delayed impingement. The ratio of cross-flow velocity to jet velocity is defined as blow ratio, which express the strength of cross-flow. Cross-flow can be developed from a free stream in the direction perpendicular to jet or wall jet formed from the spend air from neighbouring impinging jets. Florschuetz *et al.*, [9-10] and Florschuetz and Su [11-12] investigated the effect of the initial cross-flow on flow characteristics and heat transfer. They observed the dominance of initial cross-flow with larger h/D ratio. They also observed the decrease in overall heat transfer coefficient due to initial cross-flow. Better uniformity in heat transfer was reported by Chambers *et al.*, [13] with the aid of initial cross-flow, at the expense of peak Nusselt number.

Several research articles published recently were primarily focused towards the simulation of jet impingement, which can replace the complex experiment procedures. Employing standard commercial CFD packages, Spring et al., [14] and Xing et al., [15] numerically predicted the heat transfer characteristics of jet impingement configurations with maximum cross-flow. Efficacy of various turbulence models were examined by several researchers. Comprehensive analysis of these models for multiple impinging jet system was surveyed by Shukla and Dewan [16], Rao et al., [17] and Zu et al., [18]. They reported that, SST  $k-\omega$  turbulence model is the best model for predicting the turbulence at different regimes of jet impingement, wall jet, and fountain flow. Angioletti et al., [19] evaluated the fitness of different types of turbulence models through comparative study between experimental and numerical results. It is revealed that for lower Reynolds number, SST  $k-\omega$  is the best model while RSM and k- $\varepsilon$  RNG models offered superior performance at high Reynolds number. Pamitran et al., [20] carried out various experiments about the heat transfer coefficient of two-phase flow boiling in a mini channel tube. Idris et al., [21] developed a computational fluid dynamic model based on distributor cooling plates using Ansys to study the effect of different ratios of nano-fluids to heat transfer enhancement and fluid flow. Sidik et al., [22] explored the pressure drop in Bag Filter by varying inlet angles.

Several heat transfer enhancement techniques were experimented in conjunction with jet impingement by introducing ribs, twist tapes, baffles, dimples etc. Rao *et al.*, [23] investigated the heat transfer rate from a jet impingement over a test plate with *W*-shaped micro ribs under maximum



cross-flow situation. Their results showed that area average heat transfer rate for ribbed plate is improved by 9.6% at a jet Reynolds number of 30000. Dutta and Dutta [24] experimentally investigated frictional loss and heat transfer characteristics of turbulent flow in a constant flux heating rectangular channel with inclined baffles from the top surface. Size, position, and orientation of baffles are considered as major influencing factors in this study. They observed the influence of baffle orientation on heat transfer and peak of Nusselt number happens in the vicinity of baffles. It is also found that, friction factor decreases with decrease in the angle of baffle and with increase in perforation density. Khan *et al.*, [25] investigated the heat transfer with turbulent flow from rectangular channel with solid and perforated baffles combined with ribs. They have noticed 326% increases in heat transfer at a cost of pressure drop as high as 250%.

From the literatures, it can be concluded that, factors governing the heat transfer were well investigated. It has been revealed that the effect of cross-flow reduces the heat transfer significantly. As the occurrence of cross-flows are inevitable in jet impingement, no researches have been identified so far to utilise the cross-flow for the heat transfer augmentation with the insertion of baffles, screens or vortex generators in multi jet impingement according to best knowledge of the authors.

In the present study, heat transfer and fluid dynamics characteristics of baffle assisted multi-jet impingement with confinement and initial cross-flow was investigated using numerical simulations and experiments. Two baffle configurations (segmented and louvered baffle configurations) were compared and analysed. Louvre angle was fixed as 15°. Four baffles are arranged in each configuration to facilitate zigzag movement for cross-flow. Numerical investigation was validated against physical experiments performed on segmented baffles for various blow ratio and h/D. The influence of baffle clearance and blow ratios on heat transfer and flow dynamics were investigated in this research. Jet array contains nine circular nozzles arranged in 3×3 inline matrix. Constant velocity flow conditions are provided at the nozzle exit.

## 2. Experiment Setup and Procedures

Figure 1 shows the schematic diagram of experimental setup. The facility consists of a 3 HP blower fan, diffuser plenum, flow straighteners, cross-flow section, orifice meters, air pre-heater with temperature controllers, jet and target plates, thermocouples, DAQ system to measure temperature. All flow and temperature measuring devices are NABL calibrated.

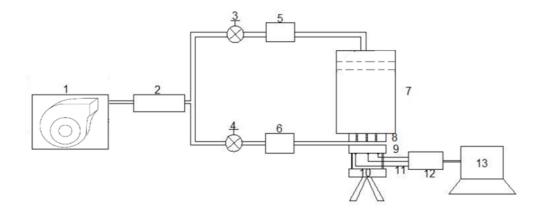
Air from the atmosphere is drawn using the blower and brought to a constant temperature of 300 K. It is then supplied to a plenum chamber to obtain the jet flow. Ambient temperature recorded at the blower inlet was in between 273 K and 297 K. Preheated air is split into two fractions and one fraction is supplied to plenum chamber fitted with two-layer honeycomb flow straighteners and nozzle plate. Nozzle plate consists of nine nozzles arranged in 3×3 inline matrix. Flow velocity at the exit of nozzles is 38 m/s and is confirmed using pitot static tube fitted to a digital manometer.

Second fraction of the preheated air is utilized for cross-flow for the test section. Calibrated orifice meters were used to measure the flow rate toward plenum chamber and cross-flow. Cross-flow is introduced normal to the jet through a tapered rectangular duct. The target plate made of Aluminium with a dimension 120 mm x 120 mm and is attached with a 50 W foil type heater at its bottom. Surface temperature of the target plate at 18 locations is measured using K-type thermocouples of accuracy  $\pm$  0.5 K.

At an interval of 1 second, real time surface temperatures are recorded using 18 channels, 12-bit data acquisition system (DAQ) and a personal computer. Height between the nozzle exit plane and



target plate surface is precisely fixed using an *X*- traverse mechanism. Uncertainty estimated in jet velocity is ±5.38 %.



- 1. Centrifugal Blower (3 hp) 2. Pre-heater 3& 4. Flow control valves, 5&6. Orifice meters
- 7. Plenum Chamber 8. Nozzle plate 9. Target plate 10. X-traverse 11 Thermocouples 12. DAQ
- 13. Computer

Fig. 1. Schematic diagram of experimental setup

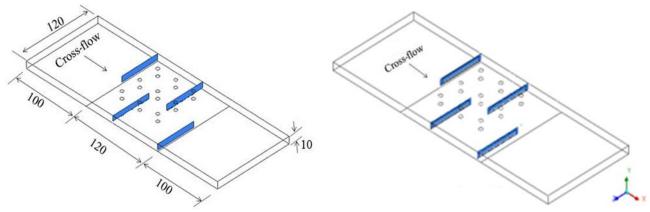
At constant jet velocity, experiments were performed at different cross-flow velocities so as to have blown ratios of 0.125, 0.25, 0.5, 0.75 and 1.0. Four baffles are provided in zigzag pattern above the target surface in the direction normal to the cross-flow. A clearance of 1, 2, and 3 mm is provided between target surface and baffle. Length of each baffle is 60 mm, which is half length of the target plate. Insertion of half-length baffles increases the turbulence over the target surface. Space between the jet plate and target surface considered is varying from 2D to 3.5D. Experiments were conducted for the validation of numerical investigation and it was done with segmented baffle configuration. Experimentations were repeated three times under similar conditions to confirm the repeatability of observations.

## 3. Numerical Modelling

Segmented and louvered baffle configurations were considered and the predictions compared with each other. The wireframe of the both configurations considered are shown in the Figure 2. The physical domain considered is a three-dimensional space with a 3 x 3 jet array over a heated plate. The domain is extended on both sides to prevent any disturbance due to boundary condition over the heated plate. The baffles are arranged in a zigzag pattern so that the cross-flow can be utilised efficiently in transferring the heat. The heated plate is of dimension 120 mm x 120 mm. Centre to centre distance between the jets in the array is 30 mm.

In the louvered baffles configuration, perforated baffles of dimension 54 mm  $\times$  5 mm, with 15° angled slat fixed on the top of perforation is used. The slat directs fluid towards the target surface. This ensures that the cross-flow is less obstructed and hence the pressure drop can be reduced. Figure 3 shows the enlarged view of baffles in two configurations. Jet enters the domain normal to the target plate with a velocity of 38 m/s, while cross-flow enters parallel to target surface from one side and leave through opposite side. Air temperature is kept at 300 K for both jet and cross-flow. The right boundary is treated as a pressure outlet kept at atmospheric pressure. The heated plate provided a heat flux of 3472.22 W/m². All other enclosing boundaries are treated as wall.

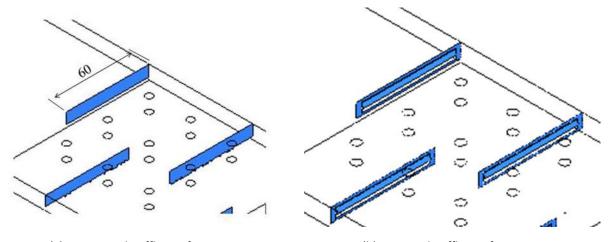




(a) Segmented Baffle Configuration

(b) Louvered Baffle Configuration

Fig. 2. Wireframe model of segmented and louvered baffle configuration



(a) Segmented Baffle Configuration

(b) Louvered Baffle Configuration

Fig. 3. Enlarged view of segmented and louvered baffle configuration

Both the air flow from jet as well as cross-flow is assumed to be incompressible, viscous, and steady. The fluid parameters like viscosity, thermal characteristics etc. are assumed to be constant. Also, no external body forces like gravity are considered. The primary heat transfer mechanisms are conduction and convection and hence radiation is neglected.

Numerical simulations were performed using commercially available ANSYS Workbench 16. Hexahedral mesh was used for discretizing the geometry keeping maximum Y+ less than 1.15 for louvered configuration and 2.5 for segmented configuration.

Second order discretization scheme was used for the pressure, continuity, momentum, energy, turbulence kinetic energy, and specific dissipation rate. Pressure Velocity coupling is carried out using SIMPLEC algorithm and SST k- $\omega$  turbulence model was selected for the present study, as it provides an acceptable harmony between accuracy and computational time. Steady state simulations were used until the solution was converged.

Grid independency test is carried out in order to discover the optimum grid size. Six different grid sizes were tested to find out the effect on the surface averaged Nusselt number and it has been found that there is no significant change in Nusselt number beyond the number of cells of 772518 for segmented configuration and 1777955 for louvered configuration as illustrated in the Table 1.



**Table 1**Grid Independence

Segmented	No of Cells	1029220	1262337	1497197	1633892	1772518	1811143.9
Configuration	Surface averaged Nu	45.2	46.7	48.5	50.4	51.0	51.1
Louvered	No of Cells	1448155	1524374	1604604	1689057	1777955	1866853
Configuration	Surface averaged Nu	33.1	34.2	35.2	36.4	37.1	37.2

#### 4. Validation

Numerical results are validated against experimental observations and results are shown in Figure 4. Comparison has been made with the numerically predicted temperature and experimental results at selected points on target plate for a baffle clearance of 1 mm and blow ratio of 0.75. It is observed that experimental observations and numerical prediction are in good agreement with a maximum variation limited to  $\pm 2^{\circ}$ C.

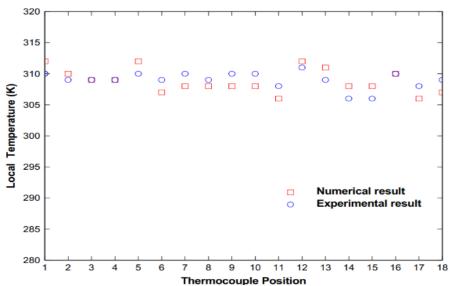


Fig. 4. Validation of numerical values with experimental results

#### 5. Results

## 5.1 Comparison of Segmented and Louvered Baffle Configurations

It is well established that provision of baffles at the beginning of heated surface disturbs the boundary layer development with consequent improvement of heat transfer [21]. Two different configurations of baffle assisted jet impingement systems were considered and a comparative study is presented here. First configuration is segmented baffles and second configuration is baffles with louvers. Figure 5 shows temperature contours of heated plate at various blow ratios for both configurations. At low blow ratios, effect of jet impingement heat transfer is visible at all jet positions except at centreline of leading edge. At this particular region, flow deflection towards this region caused by resistance of second set of baffles weakens jet impingement. It is also observed that, high temperature regions are less for configuration-1 compared to configuration-2.



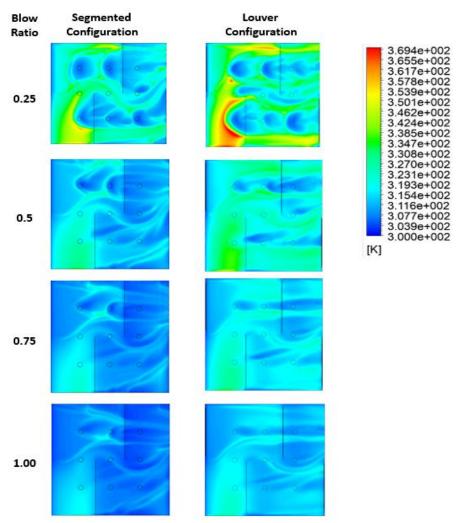


Fig. 5. Temperature contours for various blow ratios

Axial velocity contours on heated surface of both configurations for blow ratio 0.25 shown in Figure 6, indicates that higher velocities are experienced by segmented configuration compared to louvered configuration. Enhancement of fluid velocities at locations just downstream of baffles in segmented configuration is primarily due to obstruction that results in convergence of streamlines underneath of baffles. Higher flow resistance caused by baffle results in increased air flow through the clearance between baffle and bottom surface. However, in louvered configuration, perforation allows air flow through it, thereby limiting the convergence of streamlines. Higher flow velocities cause higher convective heat transfer rates that lead to lower the average surface temperature.

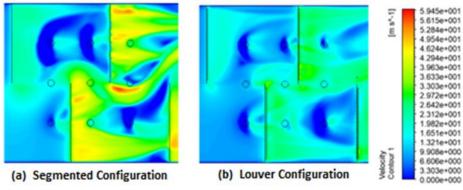


Fig. 6. Velocity contour at a blow ratio of 0.25 with baffle clearance of 2 mm



However, high velocities downstream of baffles in segmented configuration at higher blow ratio may tend to sweep away the impinging jets, consequently decreasing heat transfer by jets. However, this sweep away is very much dependant on formation of vortices behind the baffles as illustrated by Figure 7. For blow ratio 0.5, it is found that, incoming jets may deflect towards upstream if strong recirculation regions are developed behind baffles. This further weakens jet impingement. However, in louvered configuration, recirculation zones are developed closer to top confinement surface, and thus interaction with incoming jets are minimum. Therefore, it is understood that convective heat transfer mechanism causes significant heat transfer in segmented configuration while, jet impingement heat transfer is more in louvered configuration.

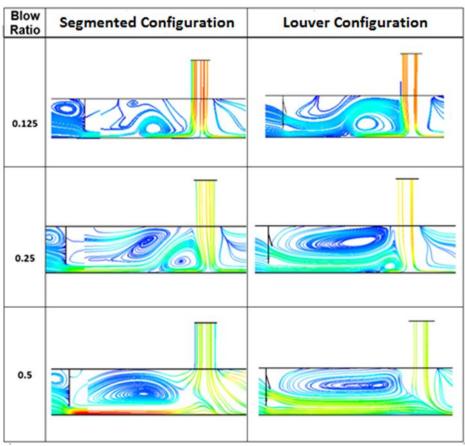


Fig. 7. Streamline distribution of Configuration 1 and Configuration 2 for h/D = 2, and clearance of 2 mm for various blow ratio

### 5.2 Nusselt Number and Pressure Drop Predictions

Trend of Nusselt number and pressure drop for segmented and louvered configuration at h/D =2 and clearance 2 mm is depicted in Figure 8. As blow ratio increases, both Nusselt number and pressure drop increases at a faster rate for segmented baffle compared to louvered arrangement. From heat transfer view, segmented baffles offer more cooling, however, pressure drop penalty is significant. Louvered baffles provide relatively lower heat transfer coefficient, but at minimum pressure drop. Therefore, performance and selection of each configuration relies upon thermal or hydraulic performance as required by the system.



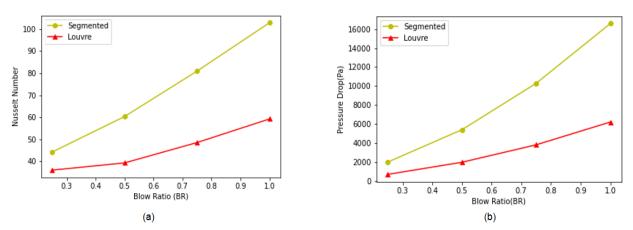


Fig. 8. Variation of Nusselt number and pressure drop for segmented and louvered baffle configuration at h/D = 2 and clearance of 2 mm

Figure 9 illustrates Nusselt number and pressure drop variation with respect to baffle clearance for segmented and louvered configuration at h/D=2 and a blow ratio of 0.25. Segmented configuration registered observable reduction in Nusselt number and pressure drop, as clearance between heated plate and baffle is increased. This is due to relatively lower velocities in the vicinity of heated surface and reduced flow obstruction that results in relatively weak recirculation zones. Louvered configuration however shows meagre changes in both heat transfer and pressure drop performance, as clearance increases. It is found that, for louvered configuration Nusselt number changes by 2.5% as clearance is increased from 1 mm to 3 mm, while Nusselt number is varied by 14% for segmented configuration. Thus, baffle clearance is not a significant operational parameter if louvered configuration is under consideration.

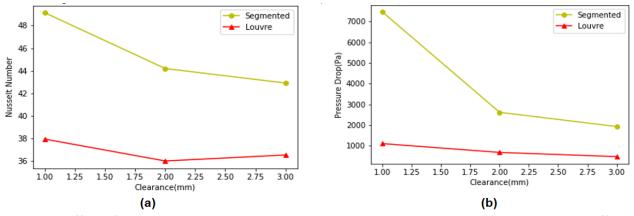
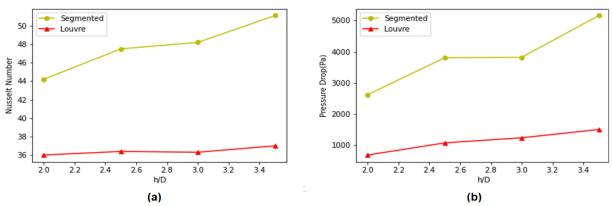


Fig. 9. Effect of clearance on Nusselt number and pressure drop, on segmented and louvered baffle configuration systems at h/D = 2 and blow ratio of 0.25

Figure 10 depicts increasing trend of Nusselt number and pressure drop as h/D ratio increases, on segmented and louvered configurations. However, the rate of variation of both thermal and hydraulic parameters is less pronounced for louvered configuration.





**Fig. 10.** Variation of Nusselt number and pressure drop for distinct h/D, on segmented and louvered configuration systems at clearance 2 mm and blow ratio of 0.25

Above discussions clarifies that, the Nusselt number obtained for segmented configuration was higher compared to louvered configuration for fixed parameters such as blow ratio, baffle clearance, and h/D. Therefore, from a thermal perspective, segmented configuration is relatively superior. However, the segmented configuration also results in a higher pressure drop in every case thus showing a dip in hydraulic performance. To justify how much pressure drop is acceptable compared to increase in heat transfer rate, Thermal Hydraulic Performance Parameter,  $\eta$  is defined as:

$$\eta = \frac{(N_u/N_o)}{(P_u/P_o)^{(\frac{1}{3})}} \tag{1}$$

where,  $N_u$  and  $N_o$  represent Nusselt number with and without baffle while  $P_u$  and  $P_o$  are the corresponding pressure drop with and without baffles respectively.

Figure 11 shows variation of thermo-hydraulic performance parameter with blow ratio for a fixed clearance of 2 mm and h/D=2. In general, performance parameter increases with blow ratio. It is found that performance parameter is improved by 86% for segmented configuration and 32% for louvered configuration as blow ratio gets increased from 0.25 to 1.0. Louvered configuration is found to be better choice for impingement systems with low values of blow ratio, while segmented configuration provides superior thermo-hydraulic performance for higher blow ratio.

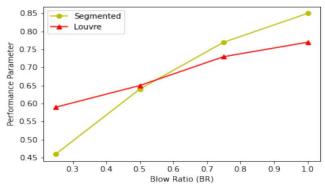


**Fig. 11.** Effect of blow ratio on Thermo-Hydraulic Performance parameter



Numerical prediction of thermo-hydraulic performance parameter with distinct values of clearance at blow ratio of 0.25 is plotted in Figure 12. Observations indicate that, performance parameters increase almost linearly with baffle clearance, for segmented and louvered configurations. Lower values of clearance provide good heat transfer rate, at the expense of significant pressure drop. Therefore, moderate clearance is preferred to obtain a good balance between thermal and fluid dynamics performance. Figure 13 shows parametric variation of performance parameter with h/D. In general, performance parameter decreases as h/D increases. In the investigated range of h/D, it is observed that a definite change in h/D causes significant change in pressure drop while resulting in insignificant changes in Nusselt Number as illustrated in Figure 10. However, it is noted that, this variation is significant for louvered configuration compared to segmented configuration. This is due to near constancy of surface averaged Nusselt number and thereby compelling increase of pressure drop of louvered configuration as h/D is increased.

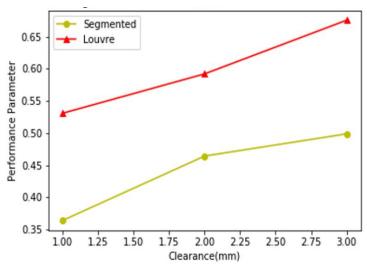


**Fig. 12.** Effect of clearance on Thermo-Hydraulic Performance parameter for blow ratio of 0.25 and h/D=2

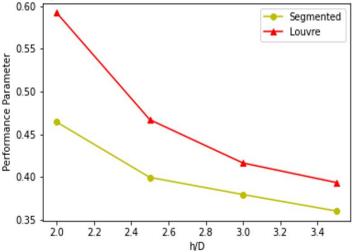


**Fig. 13.** Effect of h/D on Thermo-Hydraulic Performance parameter for clearance 2 mm and blow ratio of 0.25



#### 6. Conclusions

Jet impingement systems with segmented and louvered baffle configurations were studied and compared in terms of heat transfer and pressure drop characteristics. Heat transfer by segmented configuration is higher than louvered configuration for all blow ratios. Higher heat transfer in segmented configuration is due to higher convective heat transfer by cross-flow near to heated surface under high blow ratio conditions. However, pressure drop in segmented systems are significantly high despite of improvement in heat transfer. Louvered configuration resulted in comparatively diminished pressure drop and heat transfer. Parametric studies on thermal and hydraulic performance of baffle assisted jet impingement systems showed that; performance parameter is higher for louvered configuration only at low blow ratio. When cross-flow velocity is comparable with jet velocity, segmented baffles may be preferred because of its higher heat transfer rate relative to the incurring pressure drop. An increase in clearance proportionally increases performance parameter. However, as jet to plate distance increases, thermo hydraulic performance declines significantly.

## **References**

- [1] Freidman, S. J., and Mueller, A. C. "Heat Transfer to Flat Surfaces", *Proc. Gen. Disc. on Heat Transfer, Institution of Mech. Engineers, London*.(1951): 138-142.
- [2] Jambunathan, K., E. Lai, MAm Moss, and B. L. Button. "A review of heat transfer data for single circular jet impingement." *International journal of heat and fluid flow* 13, no. 2 (1992): 106-115. <a href="https://doi.org/10.1016/0142-727X(92)90017-4">https://doi.org/10.1016/0142-727X(92)90017-4</a>
- [3] Gauntner, James W. Survey of literature on flow characteristics of a single turbulent jet impinging on a flat plate.

  National Aeronautics and Space Administration, 1970.
- [4] Tani, Itero, and Yasuo Komatsu. "Impingement of a round jet on a flat surface." In *Applied Mechanics*, pp. 672-676. Springer, Berlin, Heidelberg, 1966. <a href="https://doi.org/10.1007/978-3-662-29364-5">https://doi.org/10.1007/978-3-662-29364-5</a> 88
- [5] Goldstein, Richard J., A. I. Behbahani, and K. Kieger Heppelmann. "Streamwise distribution of the recovery factor and the local heat transfer coefficient to an impinging circular air jet." *International journal of heat and mass transfer* 29, no. 8 (1986): 1227-1235. <a href="https://doi.org/10.1016/0017-9310(86)90155-9">https://doi.org/10.1016/0017-9310(86)90155-9</a>
- [6] Hollworth, B. R., and S. I. Wilson. "Entrainment effects on impingement heat transfer: Part 1 Measurements of heated jet velocity and temperature distributions and recovery temperatures on target surface." *Journal of Heat Transfer* 106, No 4, (1984):797-803. https://doi.org/10.1115/1.3246754
- [7] Hansen, L. G., and B. W. Webb. "Air jet impingement heat transfer from modified surfaces." *International journal of heat and mass transfer* 36, no. 4 (1993): 989-997. https://doi.org/10.1016/S0017-9310(05)80283-2
- [8] Weigand, B, and Spring, S. "Multiple jet impingement A review", *Heat Transfer Research* 42, No. 2, (2011):101-142. <a href="https://doi.org/10.1615/HeatTransRes.v42.i2.30">https://doi.org/10.1615/HeatTransRes.v42.i2.30</a>
- [9] Florschuetz, L. W., D. E. Metzger, C. C. Su, Y. Isoda, and H. H. Tseng. "Jet array impingement flow distributions and heat transfer characteristics. Effects of initial crossflow and nonuniform array geometry.[gas turbine engine component cooling]." NASA-CR-363, (1982): 1-170.
- [10] Florschuetz, L. W., D. E. Metzger, and C. C. Su. "Heat transfer characteristics for jet array impingement with initial crossflow." *ASME J. Heat Transfer* 106, (1984): 34-41. https://doi.org/10.1115/1.3246656
- [11] Florschuetz, L. W., and Cheng Su. "Heat transfer characteristics within an array of impinging jets. Effects of crossflow temperature relative to jet temperature." *NASA-CR-3936*, (1985): 1-149.
- [12] Florschuetz, L. W., and C. C. Su. "Effects of crossflow temperature on heat transfer within an array of impinging jets." ASME J. Heat Transfer 109, (1987): 74-82. <a href="https://doi.org/10.1115/1.3248072">https://doi.org/10.1115/1.3248072</a>
- [13] Chambers, Andrew C., David RH Gillespie, Peter T. Ireland, and Geoffrey M. Dailey. "The effect of initial cross flow on the cooling performance of a narrow impingement channel." *J. Heat Transfer* 127, no. 4 (2005): 358-365.
- [14] Spring, S., B. Weigand, W. Krebs, and M. Hase. "CFD heat transfer predictions for a gas turbine combustor impingement cooling configuration." In *Proceedings of the 12th International Symposium on Transport Phenomena and Dynamics of Rotating Machinery*. 2008.
- [15] Xing, Yunfei, Sebastian Spring, and Bernhard Weigand. "Experimental and numerical investigation of heat transfer characteristics of inline and staggered arrays of impinging jets." *Journal of Heat Transfer* 132, no. 9 (2010). https://doi.org/10.1115/1.4001633



- [16] Shukla, Anuj K., and Anupam Dewan. "Flow and thermal characteristics of jet impingement: comprehensive review." *Int. J. Heat Technol* 35, no. 1 (2017): 153-166. <a href="https://doi.org/10.18280/ijht.350121">https://doi.org/10.18280/ijht.350121</a>
- [17] Rao, G. Arvind, Myra Kitron-Belinkov, and Yeshayahou Levy. "Numerical analysis of a multiple jet impingement system." In *Turbo Expo: Power for Land, Sea, and Air*, vol. 48845 (2009): 629-639. <a href="https://doi.org/10.1115/GT2009-59719">https://doi.org/10.1115/GT2009-59719</a>
- [18] Zu, Y. Q., Y. Y. Yan, and J. D. Maltson. "CFD prediction for multi-jet impingement heat transfer." In *Turbo Expo: Power for Land, Sea, and Air*, vol. 48845 (2009): 483-490. https://doi.org/10.1115/GT2009-59488
- [19] Angioletti, M., R. M. Di Tommaso, E. Nino, and G. Ruocco. "Simultaneous visualization of flow field and evaluation of local heat transfer by transitional impinging jets." *International Journal of Heat and Mass Transfer* 46, no. 10 (2003): 1703-1713. https://doi.org/10.1016/S0017-9310(02)00479-9
- [20] Akbar, Ronald, A. S. Pamitran, and J. T. Oh. "Two-Phase Flow Boiling Heat Transfer Coefficient with R290 in Horizontal 3 mm Diameter Mini Channel." *Journal of Advanced Research in Experimental Fluid Mechanics and Heat Transfer* 3, no. 1 (2021): 1-8.
- [21] Idris, Muhammad Syafiq, Irnie Azlin Zakaria, and Wan Azmi Wan Hamzah. "Heat Transfer and Pressure Drop of Water Based Hybrid Al<sub>2</sub>O<sub>3</sub>: SiO<sub>2</sub> Nanofluids in Cooling Plate of PEMFC." *Journal of Advanced Research in Numerical Heat Transfer* 4, no. 1 (2021): 1-13.
- [22] Sidik, Nor Azwadi Che, Solihin Musa, Siti Nurul Akmal Yusof, and Erdiwansyah Erdiwansyah. "Analysis of Internal Flow in Bag Filter by Different Inlet Angle." *Journal of Advanced Research in Numerical Heat Transfer* 3, no. 1 (2020): 12-24.
- [23] Rao, Yu, Peng Chen, and Chaoyi Wan. "Experimental and numerical investigation of impingement heat transfer on the surface with micro W-shaped ribs." *International Journal of Heat and Mass Transfer* 93 (2016): 683-694. <a href="https://doi.org/10.1016/j.ijheatmasstransfer.2015.10.022">https://doi.org/10.1016/j.ijheatmasstransfer.2015.10.022</a>
- [24] Dutta, Prashanta, and Sandip Dutta. "Effect of baffle size, perforation, and orientation on internal heat transfer enhancement." *International Journal of Heat and Mass Transfer* 41, no. 19 (1998): 3005-3013. https://doi.org/10.1016/S0017-9310(98)00016-7
- [25] Khan, Jamil A., Jason Hinton, and Sarah C. Baxter. "Enhancement of heat transfer with inclined baffles and ribs combined." *Journal of Enhanced Heat Transfer* 9, no. 3&4 (2002). https://doi.org/10.1080/10655130215738